

**2-D PATH CORRECTIONS FOR LOCAL AND REGIONAL CODA WAVES:
A TEST OF TRANSPORTABILITY**

Kevin M. Mayeda¹, Luca Malagnini², W. Scott Phillips³, William R. Walter¹,
Douglas S. Dreger⁴, and Paola Morasca⁵

Lawrence Livermore National Laboratory¹; Istituto Nazionale di Geofisica e Vulcanologia, Roma²;
Los Alamos National Laboratory³; University of California, Berkeley⁴; and University of Genova⁵

Sponsored by National Nuclear Security Administration
Office of Nonproliferation Research and Engineering
Office of Defense Nuclear Nonproliferation

Contract Nos. W-7405-ENG-48¹ and W-7405-ENG-36³

ABSTRACT

Reliable estimates of the seismic source spectrum are necessary for accurate magnitude, yield, and energy estimation. In particular, how seismic radiated energy scales with increasing earthquake size has been the focus of recent debate within the community and has direct implications for earthquake source physics studies as well as hazard mitigation. The one-dimensional (1-D) coda methodology of Mayeda et al. (2003) has provided the lowest variance estimate of the source spectrum when compared against traditional approaches that use direct S-waves, thus making it ideal for networks that have sparse station distribution. The 1-D coda methodology has been confined mostly to regions of approximately uniform complexity. For larger, more geophysically complicated regions, two-dimensional (2-D) path corrections may be required. We will compare performance of 1-D versus 2-D path corrections in a variety of regions. First, the complicated tectonics of the northern California region coupled with high quality broadband seismic data provide for an ideal “apples-to-apples” test of 1-D and 2-D path assumptions on direct waves and their coda. Next, we will compare results for the Italian Alps using high frequency data from the University of Genova. For northern California, we used the same station and event distribution and compared 1-D and 2-D path corrections and observed the following results: (1) 1-D coda results reduced the amplitude variance relative to direct S-waves by roughly a factor of 8 (800%); (2) Applying a 2-D correction to the coda resulted in up to 40% variance reduction from the 1-D coda results; (3) 2-D direct S-wave results, though better than 1-D direct waves, were significantly worse than the 1-D coda. We found that coda-based moment-rate source spectra derived from the 2-D approach were essentially identical to those from the 1-D approach for frequencies less than ~ 0.7 Hz; however, for the high frequencies ($0.7 \leq f \leq 8.0$ Hz), the 2-D approach resulted in inter-station scatter that was generally 10-30% smaller. For complex regions where data are plentiful, a 2-D approach can significantly improve upon the simple 1-D assumption. In regions where only 1-D coda correction is available it is still preferable over 2-D direct wave-based measures.

OBJECTIVE

The motivation behind this study was to test the averaging nature of coda waves in a region that is laterally complicated. Recently the coda methodology of Mayeda et al. (2003) was applied to micro-earthquake data sets from two sub-regions of northern Italy (i.e., west Alps and northern Appenines). Since the study regions were small, ranging between local-to-near-regional distances, the simple 1-D path assumptions used in the coda methodology worked very well. However, the lateral complexity of this region would suggest that a 2-D path correction might provide even better results, especially when paths traverse larger distances and complicated regions. The structural heterogeneity of northern Italy makes the region an ideal test area to apply a 2-D Q tomography technique and test the transportability of the 2-D methodology of Phillips et al. (2003). We will compare our results with those derived from direct waves as well as some recent results from northern California.

RESEARCH ACCOMPLISHED

Coda waves are the scattered waves that follow the geometrical arrival, often referred to as the “direct waves.” The 1-D methodology of Mayeda et al. [2003] has been successfully applied in a variety of tectonic settings where the assumption of a radially symmetric path correction was sufficient (e.g., Eken et al., 2004; Morasca et al., 2005). In general, this resulted in inter-station amplitude scatter that was 3-to-4 times smaller than the traditional approach using direct S, Lg, and surface waves.

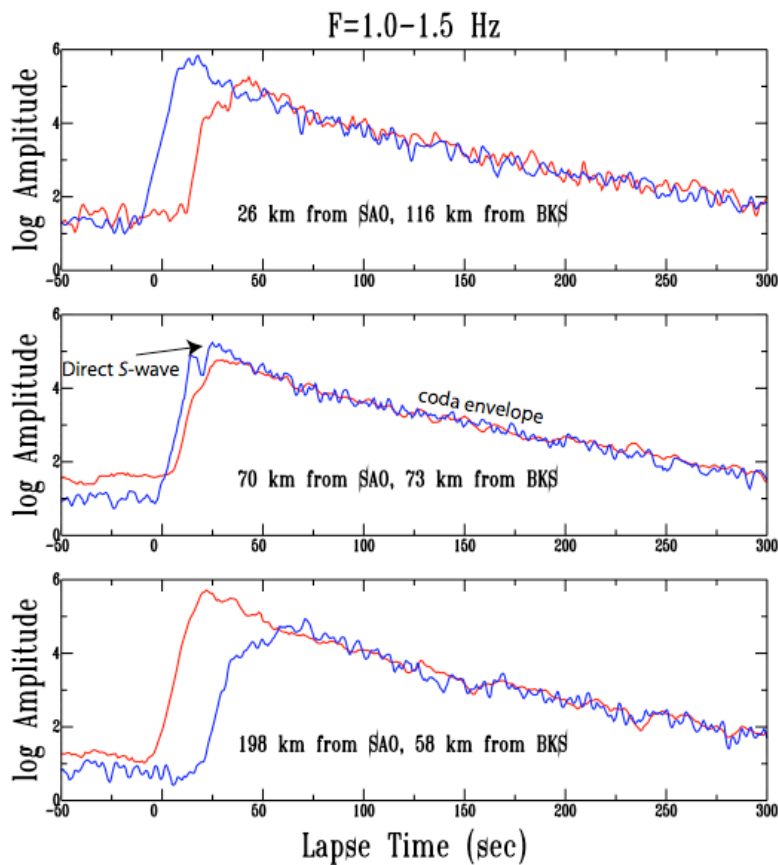


Figure 1. Example envelopes ($f=1.0-1.5$ Hz) for three events located in the San Francisco Bay region recorded at stations SAO (blue) and BKS (red), part of the Berkeley Digital Seismic Network (BDSN). At this range of distances, the scattered S-waves or “coda” is homogeneously distributed in the crust.

Figure 1 illustrates a unique property of coda waves that has been the basis of numerous studies over the past several decades, namely that the coda approaches a homogeneous distribution in space and time behind the expanding direct-wave front. In this example we show three panels of three events that are recorded at station BKS and another station, SAO, located ~140 km to the southeast. The three events were chosen such that one was relatively close to BKS, the other roughly in between, and the last event was close to SAO. In all panels we see that the coda envelope levels are approximately the same, independent of the source-station distance. This is in sharp contrast to the direct waves (S and L_g), which differ significantly in amplitude because of attenuation, geometrical spreading, and radiation pattern. Whether one believes in single or multiple scattering, isotropic or non-isotropic scattering, the observational evidence clearly shows that the crust tends to homogenize the coda energy at local-to-near-regional distances (e.g., Aki, 1969).

The previous example is in a region that is generally uniform, dominated by structures related to the coast ranges. In larger, more laterally complex regions there may be a need to extend the 1-D approach to account for 2-D variations

in structure, especially at frequencies above ~1 Hz. Phillips et al. (1998) showed that 2-D interpolated path corrections could reduce variance in regional direct phases and coda amplitudes, with the most dramatic effect on direct L_g . Recently, Phillips et al. (2003) have applied a 2-D amplitude ratio tomography to data in central Asia by assuming that the coda envelope amplitude could be idealized as if it were a direct wave, which is valid for the short segments of the early coda that they used. They performed a tomography to invert for $1/Q$ along the path, and through the choice of damping parameter and geometrical spreading, they in effect distributed the attenuation over an area, not unlike what has been previously assumed in the single-scattering model of Aki (1969) where the attenuation is attributed to an ellipsoidal volume.

Coda Measurements

The coda methodology is described in detail by Mayeda et al. (2003) so we give only a short, qualitative review here. The coda method is based upon narrowband amplitude measurements taken simultaneously from the envelope ranging from several tens of seconds up to hours depending on the frequency band and event magnitude (e.g., Mayeda and Walter, 1996). A coda envelope amplitude measurement significantly reduces the variance associated with 3-D path heterogeneity, random interference, and source heterogeneity, all of which more strongly affects the direct waves.

To form the envelopes, the horizontal velocity waveforms for each event were narrow bandpassed for 13 frequency bands ranging between 0.03 and 8.0 Hz. Envelopes were formed for each component, \log_{10} averaged for additional stability then smoothed. The coda envelopes for each frequency band can be idealized with the following equation,

$$A_c(f, t, r) = W_o(f) \cdot S(f) \cdot T(f) \cdot P(r, f) \cdot H(t - t_s) \cdot (t - t_s)^{-\gamma(r)} \exp[-b(r) \cdot (t - t_s)] , \quad (1)$$

where f is the center frequency, r is the epicentral distance in kilometers, t is the time in seconds from the origin time, t_s is the S-wave travel time in seconds, W_o represents the S-wave source, S is the site effect, T represents the S-to-coda transfer function effect, P includes the distant-dependent effects of geometrical spreading and attenuation, H is the Heaviside step function, $\gamma(r)$ and $b(r)$ are the distance-dependent coda shape factors that control the coda envelope shape. For simplicity, we have set $\gamma = 0.2$ noting that this parameter only controls the early part of the coda immediately following the direct arrival which is more influenced by source radiation pattern. Since we are fitting the coda over large amounts of time, the exponential term $b(r)$ is the most important parameter as it controls the majority of the coda envelope shape. However for the purpose of generating synthetics we set W , S , T , and P to unity. The coda shape parameters and velocity of the peak S/L_g -wave arrival were fit as a function of distance using the form of a hyperbola,

$$[\text{e.g., } b(r) = b_0 - \frac{b_1}{b_2 + r}] . \quad (2)$$

1-D Coda

The empirical 1-D path correction for coda has the property of being roughly constant up to a certain critical distance then falls off with increasing distance. This phenomenon has been observed with local and regional data (e.g., Figure 1) where the path term P in Equation 1 can be written as

$$P(r, f) = \left[1 + \left(\frac{r}{p_2} \right)^{p_1} \right]^{-1} , \quad (3)$$

where p_1 controls the amplitude decay beyond the critical distance p_2 . We used common recordings using 6 station pairs that sample the region and then grid searched over p_1 and p_2 and tabulated the interstation scatter for each frequency band. The choice of frequency-dependent path correction for the entire region was based upon the path parameters p_1 and p_2 that gave the lowest average interstation standard deviation between our 6 station pairs.

1-D Direct Waves

For every coda amplitude that was measured we also measured the corresponding peak envelope amplitude of the direct wave (e.g., S, L_g or surface waves). As done previously with the coda, we applied a grid search using the direct wave amplitudes to estimate the best value of Q. Through numerical simulation Yang (2002) showed that regional, peak envelope amplitudes decay roughly as 1/*r* so we have adopted the following formulation where the direct wave amplitude at distance *r* and frequency *f* is,

$$A(r, f) = A_0 \cdot S(f) \cdot \frac{1}{r} \cdot e^{-\left[\frac{\pi f}{\beta Q_\beta}\right]}, \quad (4)$$

where *A*₀ is the source term, *S* is the site effect, *β* is the S-wave velocity (set to 3.5 km/sec), and *Q*_β is the S-wave quality factor. We then solved for the best value of Q that minimized the scatter between the same 6 station pairs that were used for the coda path corrections. The averaged S-wave Q follows the form, *Q*(*f*) = 129 *f*^{0.57} for frequencies between 0.3 and 8.0 Hz.

2-D Corrections

For testing 2-D attenuation we elected to use amplitude ratios taken between two or more stations that recorded the same event. This avoids solving for or applying initial estimates of source terms, which results in much higher resolution images and lowers residual variance. This is simply the tomographic extension of popular methods such as the reversed two-station method (e.g., Chun et al., 1987) or the station-pair-event-pair method (e.g., Shih et al., 1994; Fan and Lay, 2003), both used to obtain a single *Q* for a sampled region. We must assume that the source radiates isotropically, which is generally true for L_g and coda, and thus, allows cancellation of source terms for rays that take off along different azimuths. We apply the following amplitude ratio formulation:

$$A_{ij} - \langle A_{ij} \rangle_j = S_i - \langle S_j \rangle_j + (P_k dx_{ijk} a_k - \langle P_k dx_{ijk} a_k \rangle_j) \log_{10}(e) \quad (5)$$

where *A* represents log₁₀ amplitude after correction for assumed 1/*r* spreading, *i, j, k*, indices represent site, source and path discretization, respectively, *S* represents log₁₀ site terms, the *dx* are path lengths through a discretized region of the Earth, *a* is the discretized attenuation coefficient (*a*_{*k*} = ω/2*Q*_{*k*}*c*) and the *P*_{*k*} represent ray path sums. The $\langle \rangle_j$ represent averages taken over all ray paths or sites associated with event *j*. The equation is obtained from (4) taking the average for event *j*, then removing the average. The source term becomes source minus the average source for event *j*, which is taken to be zero. Implementation requires sources recorded at multiple stations, as an event recorded at a single station will result in a null equation. This is a standard technique for removing source effects from an inverse problem (e.g., Aki and Richards, 1980). The equation is linear and can be solved easily using sparse matrix methods. We apply first-difference regularization (smoothness constraints) to the attenuation model and require that the site terms sum to zero to account for the non-uniqueness associated with the relative nature of the problem.

We used the same data set as in the 1-D case and assumed a cell dimension of 0.1 degree. First of all, we found that the coda results loosely followed the direct wave results in that the *Q*'s in the coast ranges were low relative to the Sierra Nevada region (Figure 2). The main difference was that the coda results rarely varied by more than a factor of 2 across the region, whereas the direct waves varied by upwards of 4-to-5 times. As expected, the direct wave *Q*'s were more sharply defined than the coda results which is likely the result of the natural smoothing of coda waves.

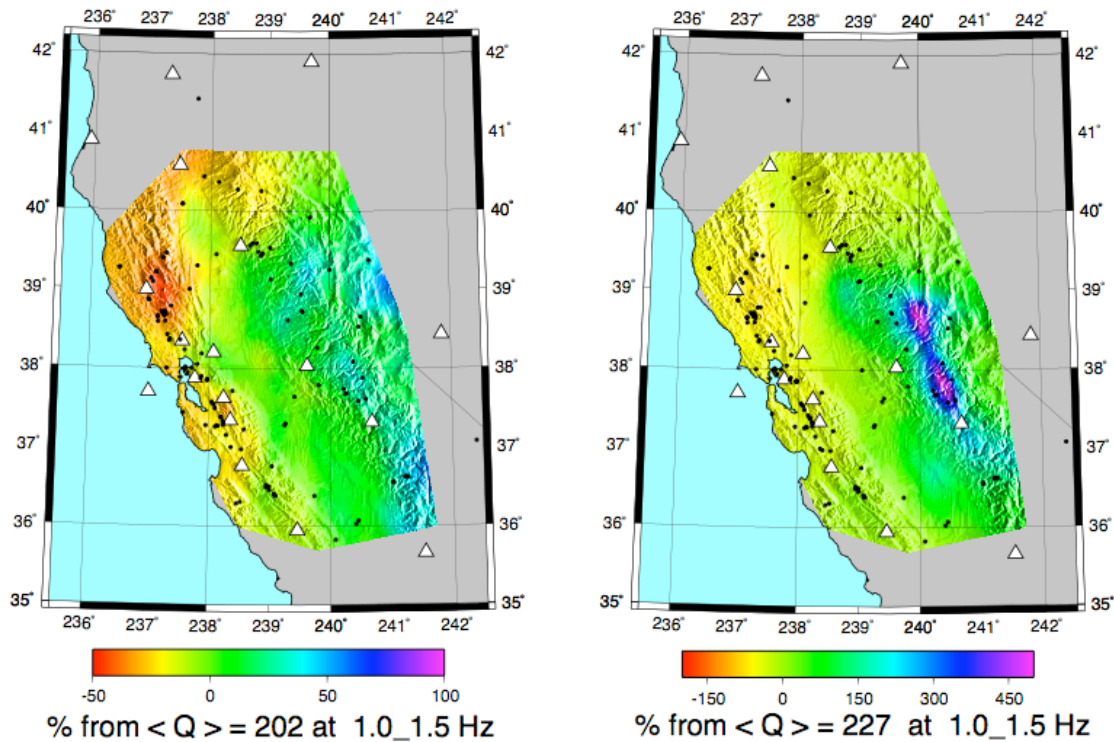


Figure 2. (a) For the 1.0–1.5 Hz case we observe coda attenuation is highest near the coast ranges and low in the Sierra Nevada region. (b) Same as in Fig. 2a except for the direct wave case. Triangles represent broadband stations and solid black circles are events used in the study. The colored portion of the map was determined by a 1-degree checkerboard test and delineates the region where we have good resolution.

COMPARISONS

We compared distance-corrected amplitudes at multiple pairs of stations to assess the performance of the four different approaches. In general, the average interstation standard deviation for the 1-D coda slowly increases from ~ 0.08 at 0.05–0.1 Hz to ~ 0.22 at 6–8 Hz whereas the scatter for 1-D direct waves resulted in an average interstation scatter that is generally a factor of 2-to-3 larger, or roughly 800% larger in variance (Figure 3). The 2-D coda results were roughly 2 times lower in scatter than 2-D direct *S*-wave results, and surprisingly the 2-D direct wave results were still much worse than the 1-D coda results. Finally, the 2-D coda results did improve the scatter relative to the 1-D case, reducing the variance by roughly 40%.

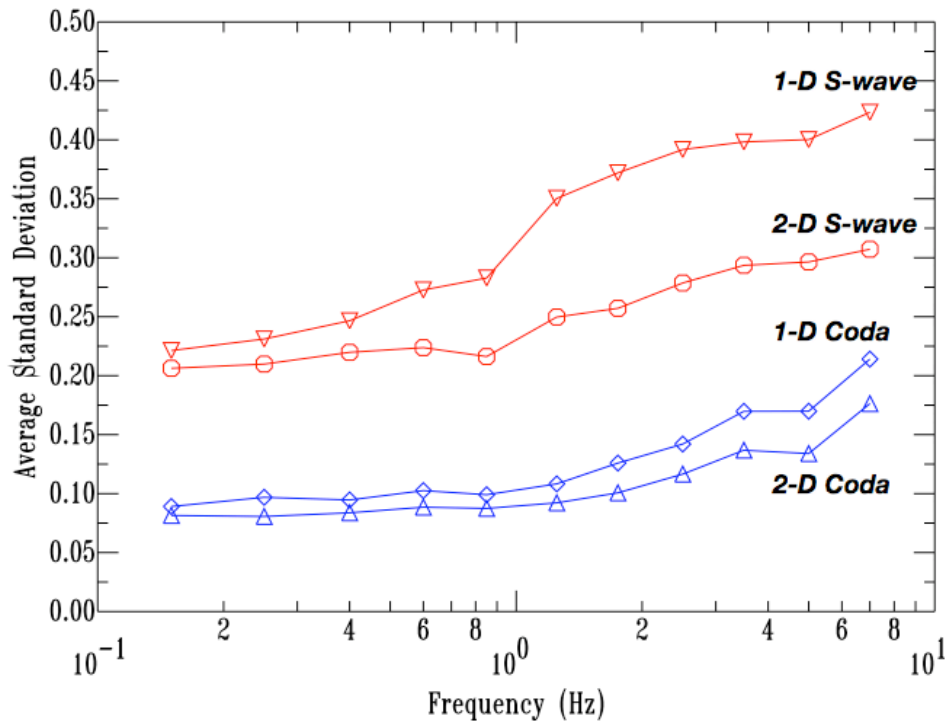


Figure 3. Averaged interstation standard deviation using 45 station pairs as a function of frequency. We see that 1-D coda are significantly less scattered than either of the direct S-wave results.

Although the coda amplitudes are corrected for frequency-dependent path effects, they still carry the S-to-coda transfer function as well as site effects that must be removed in order to obtain a moment-rate spectrum that has absolute units (e.g., dyne-cm). Again we refer the reader to Mayeda et al. (2003) for the calibration details. As found in other regions, coda-derived M_W 's from a single station were in excellent agreement with the network-averaged values. We also applied a similar transformation to remove the site effect for the direct waves and their averaged M_W 's were also in good agreement. Figure 4 summarizes results of all four methods using the M_W 5.0 Napa earthquake of September 3, 2000, as an example. Though more scattered, the average of the direct wave spectra is very similar to the individual coda spectra, thus proving the point that a single-station coda spectra is equivalent to a network average using direct waves. The stability of the coda-derived spectra is remarkable considering they are derived from different azimuths and distances, mixing local S-wave, regional L_g , and surface wave codas.

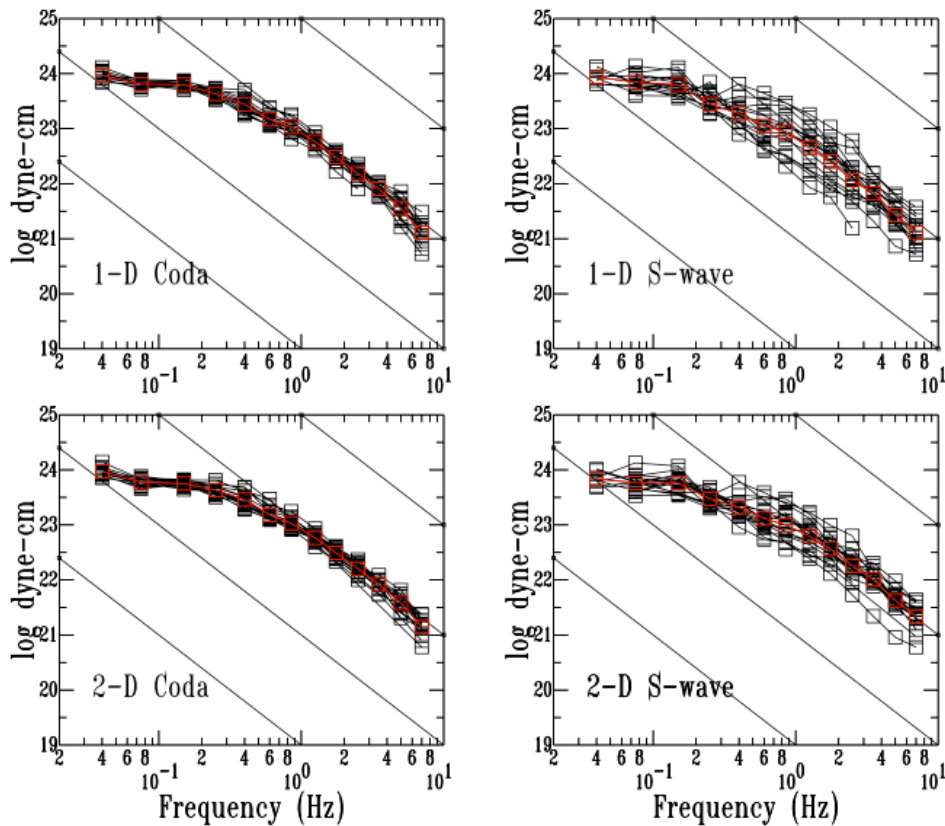


Figure 4. Moment-rate spectra for the M_W 5.0 Napa earthquake of September 3, 2000. Black lines represent individual station spectra and red lines represent the average. Stations are situated at a variety of azimuths and range between a few 10's of kilometers to over 400 kilometers.

In addition to stable single station estimates of M_W , the coda spectra shown in Figure 4 can also be used to obtain reliable estimates of the radiated energy (E_R) (e.g., Mayeda and Walter, 1996; Mayeda et al., 2005). Ide and Beroza (2001) reviewed a number of scaled energy $\tilde{\epsilon}$ ($=E_R/M_0$) studies from around the world and concluded that the large scatter did not support $\tilde{\epsilon}$ changing as a function of increasing M_0 . We found dramatic regional differences in $\tilde{\epsilon}$ for events with the same M_W . For example, events in and around the Geysers have anomalously low corner frequencies and low $\tilde{\epsilon}$ in sharp contrast to events in the Gilroy and Sierra Nevada regions which have much larger corner frequencies and larger high frequency amplitudes. This finding could not be explained by low Q in the Geysers region and points to a difference in rupture dynamics for these events. This illustrates the potential problem of combining $\tilde{\epsilon}$ for events over a broad region because the scatter of $\tilde{\epsilon}$ could make resolving scaling variations impossible. Instead, it may be more prudent to look for scaling in earthquake sequences or smaller geographical regions to avoid undue scatter (e.g., Mayeda et al., 2005).

Transportability to Northern Italy

To test the transportability of the method, we selected the same events and stations for both coda and direct S-waves in northern Italy (see Figure 5). We compared direct and coda waves using 1-D and 2-D attenuation corrections showing that the 2-D method provides more stable results than the 1-D approach for the same phase. However, when we compare direct and coda waves, we notice that the simple 1-D attenuation corrections applied to coda measurements result in more stable source spectra than those obtained using the 2-D parameters applied to direct waves. The same trend is observed for northern California, although the standard deviations are slightly larger than those in Italy for the frequency range 0.7–8.0 Hz. Moreover, we obtain a lower Q for the coda when we correct

using the 2-D attenuation. Since the study area is quite small because of the data and station distribution, for the future we will add more events and stations from other networks to enlarge the study area and better understand the relation between attenuation and geological structures.

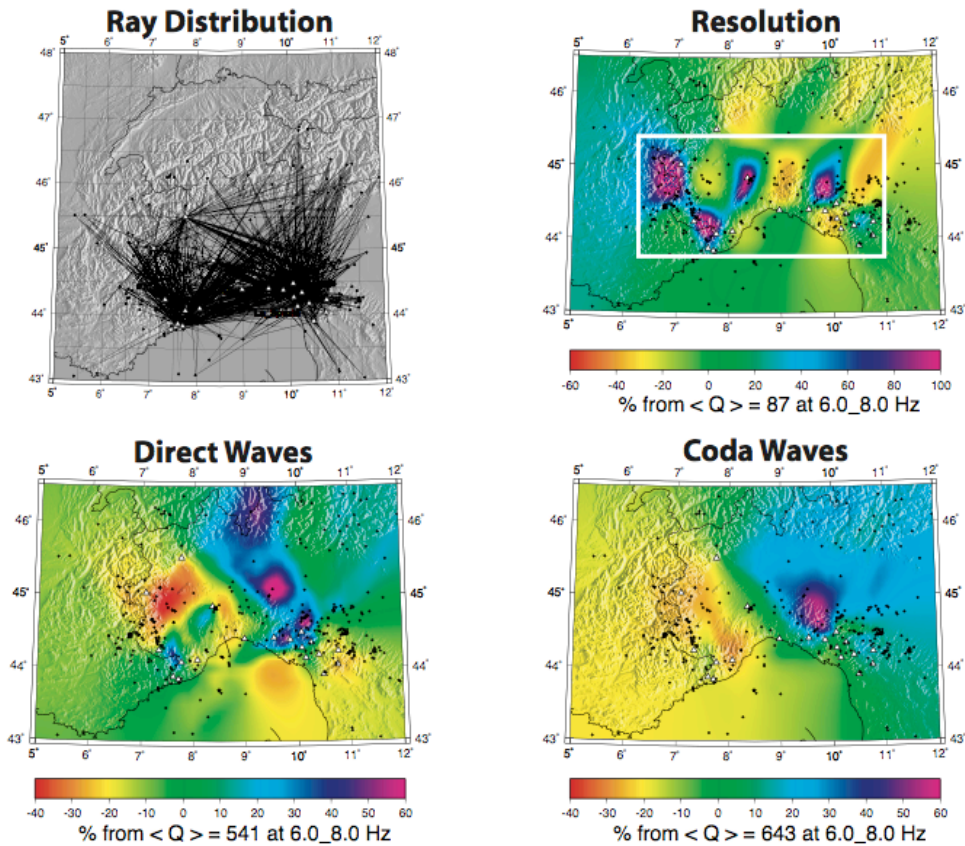


Figure 5. (a) Path map showing event and station distribution of the case of 6–8 Hz in northern Italy. (b) Result of checkerboard test using cells of 0.75 degree by 0.75 degree. White rectangle shows the region for which we believe we have good resolution. (c) The 2-D inversion results for direct waves show finer scale features. (d) Results for coda waves are smoother than those in Figure 5c but result in much lower inter-station variance, similar to California.

CONCLUSIONS AND RECOMMENDATIONS

We showed that the 2-D coda tomography methodology of Phillips et al. (2003) worked well for both northern California and northern Italy. The purpose of this study was not to exhaustively calibrate both regions for 2-D attenuation. Our goal was to perform an “apples-to-apples” test of 1-D versus 2-D path corrections using the same event and station distribution. We wanted to test the extent to which 2-D path corrections for direct waves and coda waves improved upon simple 1-D assumptions. We found that in spite of the complex structure of the region, 1-D coda results performed very well. Though additional variance reduction was obtained when we applied 2-D path corrections to the coda (~40%), these were relatively minor and come at the expense of adding ~15 degrees of freedom. Comparing direct S-wave results, we found significant variance reduction for 2-D versus 1-D results, by as much as 200% at frequencies above 1 Hz. In spite of many more degrees of freedom, the 2-D direct wave results still performed significantly worse than the simple 1-D coda. The 2-D approach for coda may be more useful in the case when there are longer path lengths and/or more significant lateral changes in crustal structure and thickness. For the northern California region however, 1-D results were perfectly adequate to derive stable source spectra and related parameters for coda.

27th Seismic Research Review: Ground-Based Nuclear Explosion Monitoring Technologies

The calibration resulted in excellent agreement with the Berkeley Seismological Laboratory's (BSL) long-period waveform-based moment magnitude estimates ($\sim 3.5 < M_w < 6.5$). Coda-based moments have the advantages that M_w 's can be measured reliably with as few as one station and for events that are too small to be waveform modeled. This last point is important because it extends the BSL's capability of computing M_w for events in the M_w 2 range throughout the footprint of the BDSN. We demonstrate in this study that the simple assumptions of frequency-dependent, 1-D path corrections are perfectly adequate for on-shore events in the northern California region.

ACKNOWLEDGEMENTS

L. Malagnini was partially funded by the Ministero dell'Universita' e della Ricerca Scientifica, MIUR, under project FIRB, Prot. RBAU013NRZ.

REFERENCES

- Aki, K. (1969), Analysis of Seismic Coda of Local Earthquakes as Scattered Waves, *J. Geophys. Res.* 74: 615–631.
- Aki, K., and P.G. Richards (1980), *Quantitative Seismology*, W. H. Freeman, San Francisco.
- Chun, K.-Y., G. F. West, R. J. Kokoski, and C. Samson (1987), A Novel Technique for Measuring Lg Attenuation: Results from Eastern Canada between 1 to 10 Hz, *Bull. Seism. Soc. Am.* 77: 398–419.
- Eken, T., K. Mayeda, A. Hofstetter, R. Gök, G. Örgülü, and N. Turkelli (2004), An application of the coda methodology for moment-rate spectra using broadband stations in Turkey, *Geophys. Res. Lett.* 31: 11, L11609.
- Fan, G. W. and T. Lay (2003), Strong Lg Wave Attenuation in the Northern and Eastern Tibetan Plateau Measured by a Two-Station/Two-Event Stacking Method, *Geophys. Res. Lett.* 30: 1530.
- Ide, S and G. C. Beroza (2001), Does Apparent Stress Vary with Earthquake Size? *Geophys. Res. Lett.* 28: 3349–3352.
- Mayeda, K., R. Gök, W. R. Walter, and A. Hofstetter (2005), Evidence for Non-Constant Energy/Moment Scaling from Coda-Derived Source Spectra, *Geophys. Res. Lett.* Doi:10.1029/2005GL022405.
- Mayeda, K., A. Hofstetter, J. L., O'Boyle, and W. R. Walter (2003), Stable and Transportable Regional Magnitudes Based on Coda-Derived Moment-Rate Spectra. *Bull. Seismol. Soc. Am.* 93: 224–239.
- Mayeda, K. and W. R. Walter (1996), Moment, Energy, Stress Drop, and Source Spectra of Western United States Earthquakes from Regional Coda Envelopes. *J. Geophys. Res.* 101: 11, 195–208.
- Morasca, P., K. Mayeda, L. Malagnini, and W. R. Walter (2005), Coda-Derived Source Spectra, Moment Magnitudes, and Energy-Moment Scaling in the Western Alps, *Geophys. J. Int.* 160: 263–275.
- Phillips, W. S., G. E. Randall, and S. R. Taylor (1998), Regional Phase Path Effects in Central China, *Geophys. Res. Lett.* 25: 2729–2732.
- Phillips, W. S., H. J. Patton, C. M. Aprea, H. E. Hartse, G. E. Randall, and S. R. Taylor (2003), Automated Broad Area Calibration for Coda Based Magnitude and Yield, in *Proceedings of the 25th Seismic Research Review—Nuclear Explosion Monitoring: Building the Knowledge Base*, LA-UR-03-6029, 1: pp. 437–444.
- Shih, X. R., K.-Y. Chun, and T. Zhu (1994), Attenuation of 1–6 s Lg Waves in Eurasia, *J. Geophys. Res.* 99: 23859–23874.
- Yang, X. (2002), A numerical investigation of Lg geometrical spreading, *Bull. Seismol. Soc. Am.*, 92, 3067–3079.